Shearing Properties of Epoxy and Epoxy Bitumen as Bonding Material of Asphalt Overlay on Ultra-High Performance Concrete Slab

Trung Quang Dinh
Faculty of Civil Engineering, University of Transport and Communications, Hanoi, Vietnam
quangtrung.mot@gmail.com

Thi Kim Dang Tran
Faculty of Civil Engineering, University of Transport and Communications, Hanoi, Vietnam
tranthikimdang@utc.edu.vn (corresponding author)

Ngoc Quy Ngo
Center for Transport Science and Technology, University of Transport and Communications, Hanoi, Vietnam
quytnct47@utc.edu.vn

Received: 4 May 2024 | Revised: 31 May 2024 | Accepted: 15 June 2024

 DOI: https://doi.org/10.48084/etasr.7734

ABSTRACT

This article discusses the results of direct shear and fatigue shear tests on epoxy resin and epoxy bitumen bonding materials. Shearing properties, including shear strength, shear stiffness, shear energy, and post-failure energy, are analyzed using results from direct shear tests at 30°C and 60°C. The fatigue tests used a direct shearing test with a pulse load of 1 Hz frequency at 60°C to analyze the fatigue life and plateau value based on the ratio of dissipated energy change versus load cycles curve. At 30°C, the shearing properties of the tested epoxy resin were approximately 60-70% higher than those of the tested epoxy bitumen. The epoxy resin possesses an outstanding advantage against the epoxy bitumen at high temperatures when applying the shear energy approach. At 60°C, the shear energy of the epoxy resin was 30.5% higher than that of the epoxy bitumen, while its shear strength and shear stiffness were 18.5% and 79% lower than those of the epoxy asphalt, respectively. The shear fatigue life of the epoxy resin after the energy method was more than ten times that of the epoxy bitumen, and its plateau value was only 10% of the epoxy bitumen. Regression analysis was also performed using fatigue shear test data to provide a fatigue shear equation in the form of an exponential function.

Keywords-UHPC bridge deck; bonding; shear energy; shear fatigue; ratio dissipated shear energy

I. INTRODUCTION

Bonding quality is the major factor that affects the performance of asphalt pavements in general and asphalt overlays on concrete in composite pavements in particular [1-5]. Poor adhesion in asphalt pavements generally leads to risks of premature defects of the asphalt overlay, such as delamination, rutting, and parabolic crack, due to the low shear resistance compared to the shear forces caused by vehicle wheel loads. Various factors affect the bonding quality of asphalt overlay on concrete bridge decks, such as temperature, bonding material type, waterproofing membrane presence, concrete deck surface texture, asphalt overlay, grid interlayer, etc. [6-10].

In [11], Ultra High-Performance Concrete (UHPC) was examined in bridge engineering, including bridge girders and bridge decks. The denser structure of the constituent materials creates a smooth and hard surface on the final UHPC products, leading to poor adhesion of UHPC slabs and asphalt pavements. The widely used solution for improving the surface texture of a UHPC deck is shot blasting. The common material for shot blasting is steel sand, whose grinding behavior and manufacturing process were analyzed in [12]. However, as shown in Vietnam's Thang Long bridge rehabilitation project, it seems that shot blasting is not sufficient to improve the bonding strength of conventional bond coats. In this project, UHPC reinforcement was used to strengthen old orthotropic steel plates before overlaying them with modified asphalt.

During project preparation, poor bonding was found in the direct shear test implemented on the cores of the polymer-modified asphalt mix on UHPC slabs with conventional bonding materials, which were bitumen emulsion and polymer-modified bitumen emulsion. No bonding strength was found under the testing temperature of 60°C, which is the temperature threshold of the asphalt surface layer in the context of hot weather in Vietnam. An epoxy resin, namely Hyper Primer (HP), was used as the bonding material in this project because its direct shearing strength is superior to other common bonding materials of bitumen and polymer-bitumen emulsions used in the testing program during the project preparation [13].

Some studies investigated the bonding and fatigue shearing performance of the interlayer between two asphalt layers using shear tests. In [14], a Leutner device and a loading rate of 50 mm.min^{-1} were used to analyze the curves of shear force versus displacement. The shear test parameters obtained were shear strength, shear stiffness, shear energy, and post-failure energy. In [15], a customized double shear testing device was used to investigate the interface fatigue performance between two asphalt concrete layers. A 50% decrease in the initial value of the interface shear stiffness was used to determine the number of loading cycles to failure and predict the fatigue law. In [16], the bonding properties of double-layered asphalt specimens were investigated using a Leutner device applying cyclic shear load. The shear fatigue life was determined using the 50% stiffness reduction method. In [17, 18], the fatigue behavior of hot mix asphalt was investigated using an energy approach with the Ratio of Dissipated Energy Change (RDEC). The RDEC approach was validated and applied successfully to the fatigue endurance limit and healing. In [19], both methods were used for shear fatigue analysis between the Open-Graded Friction Course (OGFC) and the asphalt underlying layer.

There is a limited number of studies on the shearing performance and fatigue behavior of the interlayer between the concrete or rigid base and the asphalt overlay. In [20], the pull-off and shear strength of the interlayer bond between UHPC and the asphalt overlay were investigated. The UHPC surface was treated by spreading gravel or steel ball solutions, or picking with a broom or a cutting machine or grooving. The interface bonding was a 10mm thick rubber asphalt seal. The results showed that the most effective UHPC surface treatment was picking by the cutting machine to provide maximum pull-off and shearing strength. In [21], inclined shear tests were used for the fatigue analysis of the interlayer bonding between Portland Cement Concrete (PCC) and asphalt overlay for composite pavement design purposes. The shear fatigue test was carried out in a stress control mode using a 10 Hz repeated half-sinusoidal load at 25°C. The fatigue life was determined at the point where the deviation between the measured and predicted deformation of $y = ax^b$ is less than 10.

This study focuses on the shearing properties of HP and Epoxy Bitumen (BE) as interlayer materials between UHPC and the asphalt overlay. Properties studied include shear strength, shear stiffness, shear energy, and shear fatigue.

II. RESEARCH METHODOLOGY

Direct shear tests were carried out under static conditions to determine shear strength, shear stiffness, shearing energy, and post-failure energy.

$$\tau_{SBT,max} = \frac{4*F_{SBT,max}}{\pi*\Phi^2} \quad (1)$$

where $\tau_{SBT,max}$ is the shear strength (MPa), $F_{SBT,max}$ is the maximum shear force (N), and Φ is the specimen diameter (mm^2). The stiffness of the bonding material is the slope of the linear part of the force-displacement curve divided by the initial specimen cross-sectional area.

$$k_{SBT,max} = \frac{4*F'_{SBT}}{\pi*\Phi^2} \quad (2)$$

where $k_{SBT,max}$ is the shear stiffness of the bonding layer (MPa/mm), F'_{SBT} is the slope of the linear part of the force-displacement curve (N/mm), and Φ is the specimen diameter (mm^2). The shear and the post-failure energies are the work for bonding layer break, which could be defined by a non-closed line integral of the force-displacement curve. Shear energy is defined as the area below the curve of shear force and the shear displacement from the starting point to the maximum shear force (failure point), and the post-failure energy is the one from the failure point to the point corresponding to 70% of the shear strength. Direct shear tests using pulse load were carried out for the fatigue shear characteristic. 1 Hz load frequency with a loading time of 0.1 s and 0.9 s rest time was applied. The energy approach method was applied for fatigue analysis using RDEC.

In [19], the energy approach was proposed to describe better the fatigue process of interlayer materials between the OGFC and the underlying layer. This is because each part of the energy (work) of the shear load cycles applied to the sample will contribute to the fatigue process, leading to sample failure. If the amount of work contributed at each load cycle is greater, the process that leads to sample damage will be faster. RDEC is determined by:

$$RDEC_{(i)} = \frac{|w_j - w_i|}{(j-i)*w_j} \quad (4)$$

where w_j is the dissipated energy at cycle j, w_i is the dissipated energy at cycle i, and i and j are the i^{th} and the j^{th} load cycles, respectively. As the dissipated energy is the work of the shear force (constant) of each load cycle and the corresponding displacement, $RDEC_i$ is calculated by:

$$RDEC_{(i)} = \frac{|D_j - D_i|}{(j-i)*D_j} \quad (5)$$

where D_j is the displacement due to the j^{th} load cycle, and $D_i$is the displacement due to the i^{th} load cycle. The fatigue process is described by an RDEC plot versus the number of load cycles. The plot, as shown in Figure 1, typically includes three stages, where RDEC decreases rapidly in the first, becomes nearly constant in the next, and increases in the last stage. The second stage with low and almost constant RDEC is called the plateau stage with a Plateau Value (PV) [17, 18].

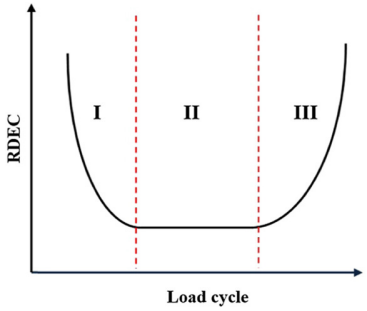

Fig. 1. Typical plot of RDEC versus number of load cycles.

III. MATERIALS FOR SHEAR TESTS

HP and BE were applied on precast UHPC slabs at a selected rate as bonding interlayer materials. Polymer-modified asphalt was overlayed on a slab specimen to simulate the UHPC bridge deck structure, bonding interlayer, and asphalt overlay. Core cylinder samples with a diameter of 100 mm taken from the slab specimen were used for shear tests. Figure 3 presents these steps. Each group included three samples of bonding material for a tested temperature. This study focused on the analysis obtained from a typical tested sample of each sample group.

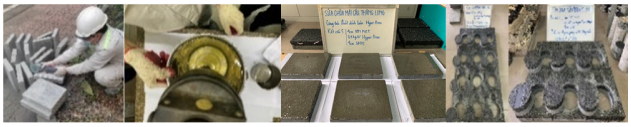

Fig. 2. Testing specimen preparation.

HP epoxy resin consists of two components: the main resin and the hardener with physical and chemical characteristics as listed in Table I.

TABLE I. HP EPOXY RESIN COMPONENTS AND CHARACTERISTICS [22]

Criteria	Properties	
	Main Resin	***Hardener***
Components	2.2,-[(1-methylethylidene) bis (4,1-phenyleneoxymethylene)] bisoxyirane homopolymer [[(2-ethylhexyl) oxy] methyl] oxyrane	(Z)-Octadec-9-enylamine 2-Propenenitrile polymer with 1.3 butadiene, 1-cyano-1-methyl-4-oxo-4-[[2-(1-piperazinyl) ethyl] amino] butyl-terminated
CAS No	25085-99-8, 2461-15-6	112-90-3, 68383-29-4
Content	50% by weight	50% by weight
Color	Fine yellow transparent liquid	Light cinnamon color liquid
Smell	Slight smell	Ammonia
Specific Gravity at 23°C, g/cm^3	1.15	0.88
Melting point, °C	< 0	0÷10
Solubility in water	Insoluble	Insoluble

The amine-based epoxy was used for BE, which consists of two components: the main resin and the hardener with properties as shown in Table II. The main resin belongs to the main group of phenolic glycidyl ether resins. The hardener is a primary amino that belongs to the group of aliphatic amines.

TABLE II. EPOXY RESIN COMPONENT AND PROPERTIES [23]

Criteria	Properties	
	Main Resin	**Hardener**
Components	1-Methylethylidene) bis (4,1-phenyleneoxymethylene) bis oxirane homopolymer	(Z)-Octadec-9-enylamine 2- Propenenitrile polymer with 1.3 butadiene, 1-cyano-1-methyl-4-oxo -4-[[2-(1-piperazinyl) ethyl] amino] butyl-terminated
CAS No	25085-99-8 5431-33-4 7460-84-6	112-90-3 68383-29-4
Content	56% by weight	44% by weight
Color	Colorless	Yellow
Smell	None	Ammonia
Specific gravity at 23°C	1.0÷1.2	0.8÷1.0
Melting point, °C	< 0	5÷10
Flash point, °C	≥ 230^{0}C	≥ 145^{0}C

The BE included the amine-based epoxy of 50% by weight, and the remaining consisted of 60/70 pen. bitumen. The properties of the BE are listed in Table III.

TABLE III. BE PROPERTIES AFTER 2-HOUR CURING

Criteria	Unit	Value
Penetration at 25°C, 5s	1/10 mm	55
Soften point	°C	63
Flash point	°C	292
Bonding with aggregate	Grade	4
Loss percentage after 5 hours heating at 163°C	%	0.3
Unit weight	g/cm^3	1.03

The UHPC for the slab specimen is the same one used to strengthen the orthotropic deck in the Thang Long bridge rehabilitation project. Table IV shows the key properties of UHPC.

TABLE IV. KEY PROPERTIES OF UHPC FOR SLAB SPECIMEN [21]

Criteria	Unit	Value
Unit weight	g/cm^3	2.43÷2.55
Compressive strength (100×120mm cylinder specimen)	MPa	≥120
Direct tensile strength (cylinder dog-bone specimen)	MPa	≥7
Elastic modulus (100×120mm cylinder specimen)	GPa	≥37.6
Slump flow (Mini cone slump - ASTM WK63516	mm	≥180 (before stabilizer mixing) ≥100 (after stabilizer mixing)

The surface texture of UHPC slab specimens after curing in special conditions was improved by shot blasting. Selected rates of BE or HP were coated evenly on the shot-blasted UHPC surface. The pull-off testing result was used for the

selected rate, which was 0.5 kg/m^2 for BE and 0.4 kg/m^2 for HP. Polymer-modified asphalt was then applied to the coated UHPC. Table V shows the design criteria of the polymer-modified asphalt.

TABLE V. POLYMER-MODIFIED ASPHALT MIX DESIGN CRITERIA FOR SPECIMEN

Criteria	Unit	Value
Unit weight	g/cm^3	2.54
Air void	%	4.52
Void of mineral aggregate	%	15.3
Void filled by asphalt	%	70.5
Marshall stability	kN	13.5
Marshall flow	mm	4.8

IV. SHEAR CURVE PARAMETERS

Shear tests using Leutner model equipment were performed to determine the shearing performance of HP and BE at 30°C and 60°C. Figure 3 shows The typical shearing curves of shear force versus displacement for HP and BE at 30°C and 60°C. As shown in Figure 3, the typical shearing curve of load versus displacement shows a high goodness of fit in the quadratic model (R^2 of around 0.99). Table VI shows the calculated parameters of the shear curve, including:

- The maximum force corresponding to the failure point is the peak of the quadratic function ($F_{SBT,max}$)
- Shear strength ($\tau_{SBT,max}$) follows (1)
- Shear stiffness ($k_{SBT,max}$) follows (2)
- Shear energy is the area below the shear curve, from the starting point to the maximum shear force
- Post-failure energy is the area below the extrapolated shear curve, from the failure point to the point corresponding to 70% of the shear strength.

TABLE VI. CALCULATED SHEAR CURVE PARAMETERS

Specimen	$F_{SBT,max}$ (N)	$\tau_{SBT,max}$ (MPa)	$k_{SBT,max}$ (MPa/mm)	Shear energy (N.mm)	Post-failure (N.mm)
UHPC-HP-30^{0}C	3,253	0.414	0.427	4,085	3,021
UHPC-BE-30^{0}C	1,952	0.249	0.260	2,379	1,759
UHPC-HP-60^{0}C	547.9	0.07	0.062	800.12	591.63
UHPC-BE-60^{0}C	649.8	0.083	0.111	612.97	453.25

In terms of shear strength, HP and BE had strengths that far exceeded the requirements specified in a technical document issued by the Japan Road Association [24]. In this document, the minimum shear strength is stipulated to be 0.15 N/mm^2 at 23°C, corresponding to a minimum displacement of 1.0 mm. This value at 30°C for HP was 0.414 N/mm^2, corresponding to a displacement of 2.5mm, and 0.249 N/mm^2 for BE at a displacement of 1.75 mm.

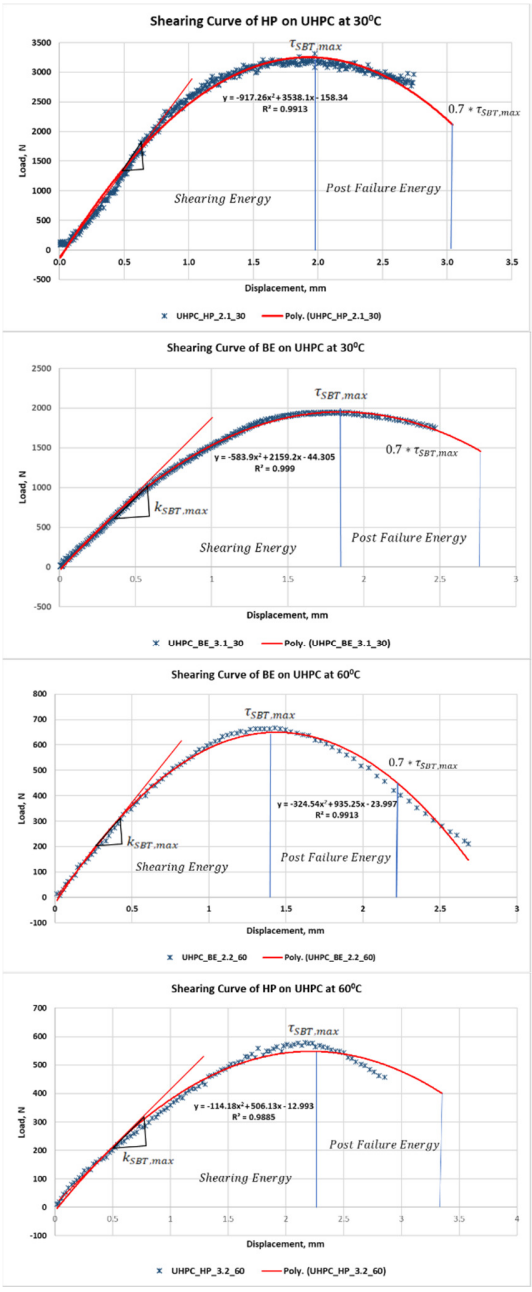

Fig. 3. Typical shear curve of HP and BE at 30°C and 60°C.

Temperature is the key factor for asphalt pavement and the interlayer between the concrete deck and the asphalt overlay. The shear parameters of epoxy resin are more temperature-dependent than those of epoxy asphalt. All HP shear parameters were less than 20% of their value when tested at a temperature of 60°C compared to those at 30°C. In particular, maximum force, shear strength, shear stiffness, shear energy, and post-failure shear energy were 16.8%, 16.9%, 14.5%, 19.6%, and 19.6%, respectively, of the tested value at 30°C. Meanwhile, the decrease in BE is less, as the values of these parameters at 60°C were 33.3%, 33.3%, 42.7%, 25.8%, and 25.8%, respectively, of the values at 30°C.

HP had better shear properties and superior shear fatigue characteristic properties than BE, especially when analyzed using the following approach. At the annual average temperature in Vietnam (i.e., 30°C), all the examined parameters of the peak shear force at the failure point exceeded those of the BE shear curve, which in turn were equal to around 60-70% of those in HP. The trend was different when analyzing the shear curve parameters at 60°C, which is the critical temperature of asphalt pavement in Vietnam's hot weather conditions. The maximum shearing force, shearing strength, and shearing stiffness of HP were lower than those of BE by 18.5%, 18.5%, and 79%, respectively. In contrast, the shear energy and the post-failure energy of HP were about 30.5% higher than those of BE. Higher energy values mean that HP could maintain shear resistance longer at a higher temperature and larger displacement. This is an outstanding advantage of the HP epoxy resin used as a bonding interlayer of the UHPC bridge deck and asphalt overlay in the hot weather conditions of Vietnam.

V. FATIGUE SHEAR CURVE

Fatigue shear tests were performed on core samples of the HP and BE interlayers between the UHPC and the asphalt overlay. The tests used Leutner model equipment with a controlled pulse load of 1 Hz frequency with a 0.1 s loading time and 0.9 s resting time. The controlled pulse load was 500 N, which is equal to 77% and 91% of the peak loads of BE (649.8 N) and HP (649.8 N), as shown in Table IV. The test temperature was 60°C. Figure 4 shows the test equipment and samples. Figure 5 shows the fatigue shear curve of BE, established for displacement versus the number of loads.

Fig. 4. Fatigue shear test device and specimens.

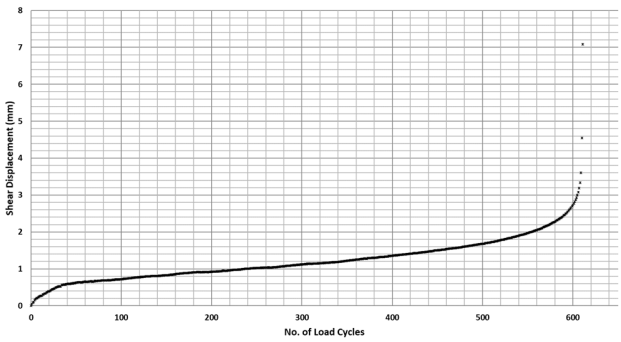

Fig. 5. Fatigue shear curve of BE at 60°C.

Figure 6 shows the plot of the RDEC versus loading cycles, indicating three stages. In stage I, the RDEC decreases rapidly as load cycles increase. In stage II, it is almost constant (PV) before accelerating in stage III when specimens fail. The PV is approximately 0.002. The shear fatigue life of BE follows the RDEC curve at the failure point at approximately the 500th load cycle, where stage III starts.

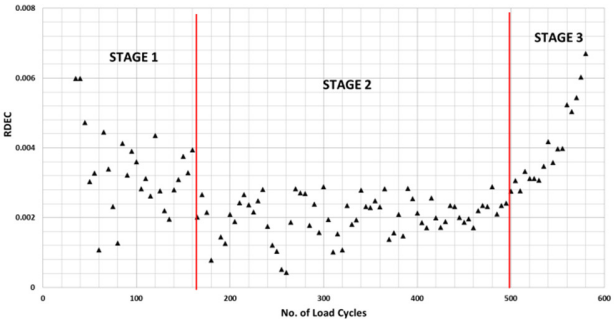

Fig. 6. RDEC of shear fatigue of BE versus load cycle at 60°C.

A regression equation was determined for the fatigue shear equation of BE at 60°C, expressed as a logarithmic function of both load cycles and displacement.

$$log_{10}(N) = 2.276 + 1.829 * log_{10}(D) \quad (6)$$

where N is the load cycle in times and D is the displacement in mm. This regression equation of load cycles and displacement provides good results of R^2 and p, (Figure 7). The non-linear regression can give a fitted exponential function (Figure 8) but with a statistically significant lack of fit. The exponential function for BE at 60°C was:

$$N = 603.972 * e^{-e^{(2.31787-2.38169*D)}} \quad (7)$$

HP fatigue shear at 60°C shows a failure point at around 6,600 load cycles, as shown in Figure 10. The shear fatigue life of HP at 60°C is more than ten times higher than BE, whereas the peak force of the failure point of HP is lower than BE.

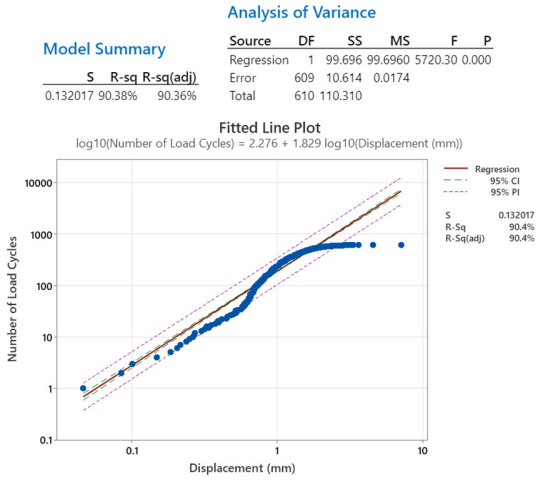

Fig. 7. Linear regression of the logarithm of load cycle and displacement.

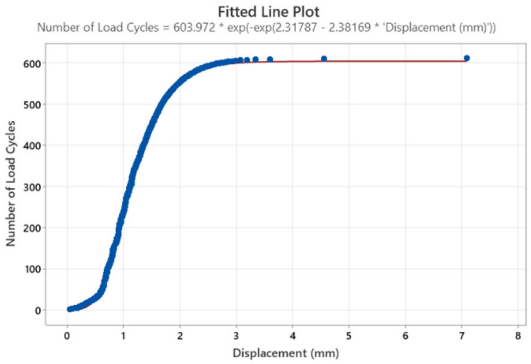

Fig. 8. Overfitted non-linear function of load cycle and displacement in the fatigue shear test of BE at 60°C.

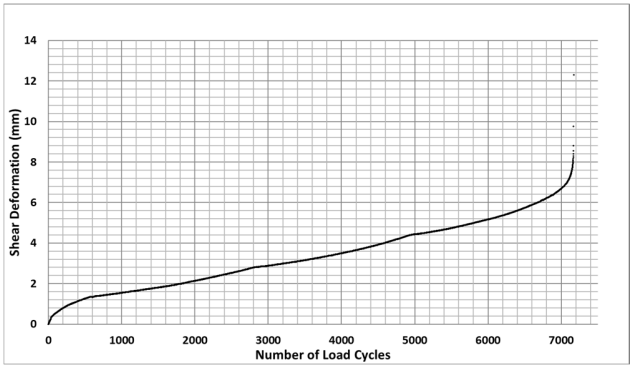

Fig. 9. Fatigue shear curve of HP at 60°C.

Figure 10 shows the plot of RDEC versus load cycles for HP, indicating the three stages. Stage II shows a nearly constant PV of approximately 0.0002, which is approximately 10% of the PV of HP at 60°C.

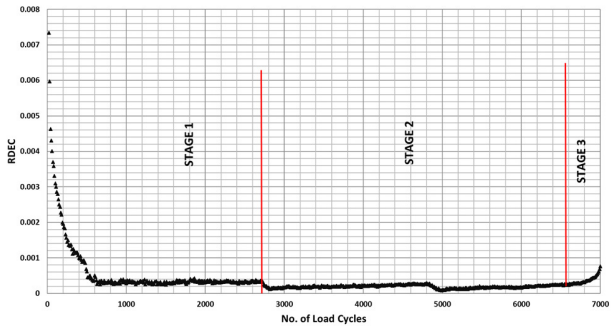

Fig. 10. RDEC of shear fatigue of HP versus load cycle at 60°C.

A similar regression was taken by adopting a fatigue shear equation of HP at 60°C, which is expressed as a logarithmic function of both load cycle and displacement.

$$log_{10}(N) = 2.630 + 1.756 * log_{10}(D) \quad (8)$$

This regression equation provides good results of R^2 and p, as shown in Figure 11.

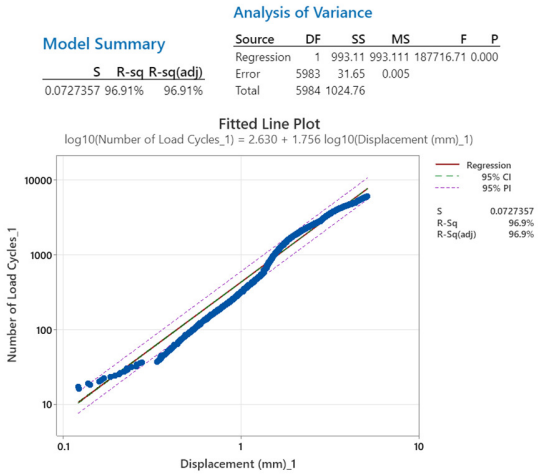

Fig. 11. RDEC of shear fatigue of HP versus load cycle at 60°C.

The exponential regression equation of HP provides a similar result to the exponential BE equation, but again, the lack-of-fit is statistically significant.

$$N = 7730.24 * e^{-e^{(1.55472 - 0.560298 * D)}} \quad (9)$$

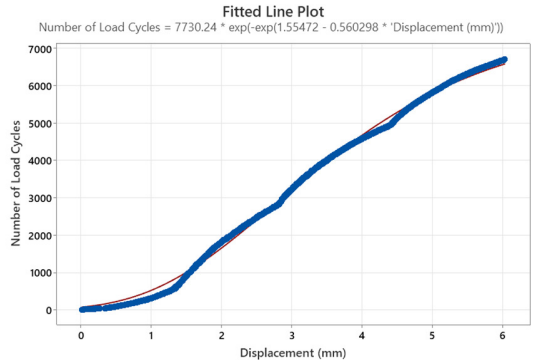

Fig. 12. Overfitted non-linear function of load cycle and displacement in the fatigue shear test of HP at 60°C.

VI. CONCLUSIONS AND RECOMMENDATIONS

The shear and fatigue shear properties were investigated for two types of interlayer materials between the UHPC deck and the polymer-modified asphalt overlay, with the epoxy resin (HP) and the epoxy bitumen (BE). The results show that both interlayers highly satisfied the shear strength requirements of the bonding between the bridge deck and the asphalt overlay. Both BE and HP can be applied as bonding interlayers between the UHPC bridge deck and the asphalt surface. The fatigue-cutting properties were also explored using the shear energy approach. The results showed that HP outperforms BE at extremely critical temperatures within the asphalt pavement, as is the case in Vietnam. As the fatigue life of HP is 13 times greater than that of BE, while its PV is only 10% to that of BE, HP is recommended as a better option for bonding the interlayer on a UHPC bridge deck in the extreme heat of Vietnam.

The shear fatigue regression equations of the investigated materials are linear functions of logarithmic load cycles versus logarithmic displacement and exponential functions of load cycles (N) and displacement (D), in the following forms:

$$log_{10}(N) = a + b * log_{10}(D)$$

$$N = \mathrm{a} * e^{-e^{(\mathrm{b}-\mathrm{c}*D)}}$$

REFERENCES

[1] A. Chabot and C. Petit, "Mechanisms of cracking and debonding in pavements: Debonding mechanisms in various interfaces between layers," *European Journal of Environmental and Civil Engineering*, vol. 21, no. sup1, pp. 1–2, Aug. 2017, https://doi.org/10.1080/19648189.2017.1361649.

[2] B. A. Hakim, "The Importance of Good Bond Between Bitaminous Layers," presented at the Ninth International Conference on Asphalt Pavements - International Society for Asphalt Pavements, Copenhagen, Denmark, Aug. 2002.

[3] M. De Beer, "Weak Interlayers Found in Flexible and Semi-flexible Road Pavements," in *8th RILEM International Conference on Mechanisms of Cracking and Debonding in Pavements*, 2016, pp. 425–430, https://doi.org/10.1007/978-94-024-0867-6_59.

[4] S. Romanoschi, "Characterization of Pavement Layer Interfaces.," Ph.D. dissertation, Luisiana State University, 1999.

[5] H. Ozer, I. L. Al-Qadi, H. Wang, and Z. Leng, "Characterisation of interface bonding between hot-mix asphalt overlay and concrete pavements: modelling and in-situ response to accelerated loading," *International Journal of Pavement Engineering*, vol. 13, no. 2, pp. 181–196, Apr. 2012, https://doi.org/10.1080/10298436.2011.596935.

[6] L. N. Mohammad, M. Raqib, and B. Huang, "Influence of Asphalt Tack Coat Materials on Interface Shear Strength," *Transportation Research Record*, vol. 1789, no. 1, pp. 56–65, Jan. 2002, https://doi.org/10.3141/1789-06.

[7] G. A. Sholar, G. C. Page, J. A. Musselman, P. B. Upshaw, and H. L. Moseley, "Preliminary Investigation of a Test Method to Evaluate Bond Strength of Bituminous Tack Coats," presented at the Technical Sessions of the Journal of the Association of Asphalt Paving Technologists. Baton Rouge, LA, USA, Mar. 2004.

[8] A. H. Albayati, N. K. Oukaili, H. Obaidi, and B. M. Alatta, "Mitigating Reflection Cracking in Asphalt Concrete Overlays with ECC and Geotextile," *Engineering, Technology & Applied Science Research*, vol. 14, no. 1, pp. 12850–12860, Feb. 2024, https://doi.org/10.48084/etasr.6650.

[9] "Optimization of Tack Coat for HMA Placement," Transportation Research Board, NCHRP 712, 2012.

[10] S. Muslich, "Assessment of bond between asphalt layers," Ph.D. dissertation, University of Nottingham, 2010.

[11] M. Zhou, W. Lu, J. Song, and G. C. Lee, "Application of Ultra-High Performance Concrete in bridge engineering," *Construction and Building Materials*, vol. 186, pp. 1256–1267, Oct. 2018, https://doi.org/10.1016/j.conbuildmat.2018.08.036.

[12] O. Bildik and M. Yaşar, "Manufacturing of Wear Resistant Iron-Steel: A Theoretical and Experimental Research on Wear Behavior," *Engineering, Technology & Applied Science Research*, vol. 11, no. 3, pp. 7251–7256, Jun. 2021, https://doi.org/10.48084/etasr.4092.

[13] "Thang Long bridge rehabilitation project, In-lab tests report," Join Venture of Transport Engineering Consultant Co. Ltd under University of Transport and Communications and TECCO2, Hanoi, Vietnam, 2020.

[14] S. C. Somé, A. Feeser, M. Jaoua, and T. Le Corre, "Mechanical characterization of asphalt mixes inter-layer bonding based on reptation theory," *Construction and Building Materials*, vol. 242, May 2020, Art. no. 118063, https://doi.org/10.1016/j.conbuildmat.2020.118063.

[15] M. Diakhaté, A. Millien, C. Petit, A. Phelipot-Mardelé, and B. Pouteau, "Experimental investigation of tack coat fatigue performance: Towards an improved lifetime assessment of pavement structure interfaces," *Construction and Building Materials*, vol. 25, no. 2, pp. 1123–1133, Feb. 2011, https://doi.org/10.1016/j.conbuildmat.2010.06.064.

[16] I. Isailović and M. P. Wistuba, "Asphalt mixture layers' interface bonding properties under monotonic and cyclic loading," *Construction and Building Materials*, vol. 168, pp. 590–597, Apr. 2018, https://doi.org/10.1016/j.conbuildmat.2018.02.149.

[17] S. H. Carpenter and S. Shen, "Dissipated Energy Approach to Study Hot-Mix Asphalt Healing in Fatigue," *Transportation Research Record*, vol. 1970, no. 1, pp. 178–185, Jan. 2006, https://doi.org/10.1177/0361198106197000119.

[18] S. Shen and S. H. Carpenter, "Dissipated energy concepts for HMA performance: fatigue and healing," Center of Excellence for Airport Technology, COE Report 29, Mar. 2007.

[19] W. Song, X. Shu, B. Huang, and M. Woods, "Laboratory investigation of interlayer shear fatigue performance between open-graded friction course and underlying layer," *Construction and Building Materials*, vol. 115, pp. 381–389, Jul. 2016, https://doi.org/10.1016/j.conbuildmat.2016.04.060.

[20] Z. Lu, Z. Feng, D. Yao, X. Li, X. Jiao, and K. Zheng, "Bonding performance between ultra-high performance concrete and asphalt pavement layer," *Construction and Building Materials*, vol. 312, Dec. 2021, Art. no. 125375, https://doi.org/10.1016/j.conbuildmat.2021.125375.

[21] T. Jin, L. Liu, R. Yang, L. Sun, and J. Yuan, "Investigation of interlayer bonding performance between asphalt concrete overlay and Portland cement concrete using inclined shear fatigue test," *Construction and Building Materials*, vol. 400, Oct. 2023, Art. no. 132681, https://doi.org/10.1016/j.conbuildmat.2023.132681.

[22] H. Nakanishi, T. Okochi, and K. Goto, "The structural evaluation for an asphalt pavement on a steel plate deck," presented at the World of Asphalt Pavements, International Conference, Sydney, Australia, 2000.

[23] "Material Safety Datasheet Consists of Resin and Hardener," Taiyu Kensetsu, Nagoya, Japan, TEJ22010EP, 2015.

[24] *Handbook for Waterproof Bridge Deck*, Japan Road Association, Tokyo, Japan, Mar. 2007.